

Scroll ring chimera states in oscillatory networks

Volodymyr Maistrenko¹, Oleksandr Sudakov^{1,2}, Ievgen Sliusar^{1,2}

¹Scientific Centre for Medical and Biotechnical Research, National Academy of Sciences of Ukraine, Volodymyrska Str. 54, 01030 Kyiv, Ukraine

² Taras Shevchenko National University of Kyiv, Volodymyrska Str. 60, 01030 Kyiv, Ukraine

E-mail: maistren@nas.gov.ua

Abstract. We report the appearance of a scroll ring and scroll toroid chimera states from the proposed initial conditions for the Kuramoto model of coupled phase oscillators in the 3D grid topology with inertia. The proposed initial conditions provide an opportunity to obtain as single as well as multiple scroll ring and toroid chimeras with different major and minor diameters. We analyze their properties and demonstrate, in particular, the patterns of coherent, partially coherent, and incoherent scroll ring chimera states with different structures of filaments and chaotic oscillators. Those patterns can coexist with solitary states and solitary patterns in the oscillatory networks.

Keywords: scroll rings, chimera states, oscillatory networks

Scroll rings appear in the models of various real physical systems and are among the most paradigmatic examples of spatio-temporal self-organizing structures in excitable media. Scroll rings occur in three-dimensional media and are formed from a scroll wave. In general, scroll rings are three-dimensional spiral waves rotating around closed one-dimensional space curves. A scroll wave is usually characterized by its filament that can be considered as the line connecting the rotation centers of the spirals in the two-dimensional cross-sections of the scroll wave. Then this filament can be closed into a ring structure called the scroll ring [1].

Scroll rings have been observed in a variety of systems including the chemical Belousov–Zhabotinsky reaction [2], in a fibrillating cardiac tissue [3], etc. The existence of a scroll ring in the media of various nature was reported as the results of numerous simulations and experiments in the fields of physics, chemistry, biology, etc. (see, e.g., [4–10]).

Chimera states [11–13] as a phenomenon of coexistence of coherent and incoherent patterns in the arrays of nonlocally coupled oscillators were investigated in a wide range of systems. For these special spatio-temporal patterns, some network’s elements oscillate synchronously with unique frequency, and the others behave themselves asynchronously. A number of articles are devoted to the theoretical and experimental studies of chimera states. Most of them deal with the models of one- and two-dimensional networks of oscillators [14].

Recently, the chimera states in a three-dimensional grid topology were investigated within various models of coupled phase oscillators [15–21]. The first report of a stable scroll ring chimera state was done in 2020 in [21] for the Kuramoto model of coupled phase oscillators in a 3D grid topology with inertia. This pattern was obtained from random initial conditions for the following equation:

$$m\ddot{\varphi}_{ijk} + \epsilon\dot{\varphi}_{ijk} = \frac{\mu}{|B_P(i, j, k)|} \sum_{(i', j', k') \in B_P(i, j, k)} \sin(\varphi_{i'j'k'} - \varphi_{ijk} - \alpha), \quad (1)$$

where $i, j, k = 1, \dots, N$, φ_{ijk} are phase variables, and the indices i, j, k are periodic modulo N . The coupling is assumed long-ranged and isotropic: each oscillator φ_{ijk} is coupled with equal strength μ to all its nearest neighbors $\varphi_{i'j'k'}$ in a ball of radius P , i.e., to those falling in the neighborhood

$$B_P(i, j, k) := \{(i', j', k') : (i' - i)^2 + (j' - j)^2 + (k' - k)^2 \leq P^2\},$$

where the distances $|i' - i|$, $|j' - j|$ and $|k' - k|$ are calculated regarding the periodic boundary conditions of the network. $|B_P(i, j, k)|$ denotes the cardinality of $B_P(i, j, k)$. The phase lag parameter α is selected from the segment $[0, \pi/2]$. The relative coupling radius $r = P/N$ varies from $1/N$ (local coupling) to 0.5 (close to the global coupling).

The parameter μ is the oscillator coupling strength, and ϵ is the damping coefficient. The parameter m is the mass. In the case $m = 0$, Eq. (1) is transformed into the 3D Kuramoto model without inertia. We put $m = 1$ without any loss of generality.

In the case of scroll ring chimera states, a filament that consists of oscillators and connects scroll waves' rotation centers has a shape of ring or toroid with different major and minor diameters in the 3D oscillatory network.

In the present paper, we propose the initial conditions for the generation of scroll ring chimera states in the Kuramoto model of coupled phase oscillators in the 3D grid topology with inertia (1). They can generate a variety of scroll ring and scroll toroid chimeras with different shapes and inner structures of their filaments. We study the properties of scroll ring chimeras and will demonstrate that they can be coherent, partially coherent, or incoherent with a hyper-chaotic behavior characterized by a number of positive Lyapunov exponents.

Scroll ring chimeras in the Kuramoto model (1) can be surrounded by solitary oscillators and can coexist with other patterns in the 3D oscillatory network. The solitary state behavior means that some number of oscillators start to rotate with a different time-averaged frequency as compared to the synchronized oscillators [21–24].

Numerical simulations were performed on the base of the Runge–Kutta solver DOPRI5 on the Ukrainian Grid Infrastructure with graphics processing units [25, 26]. In total, more than 10000 network trajectories were computed and analyzed for system (1) with $N = 100$ and 200 (1 and 8 millions of oscillators, respectively).

To obtain the scroll ring chimeras in system (1), we propose two types of the following initial conditions:

$$\varphi_{xyz} = -\theta \exp\left(-\frac{2r_{rot}}{D}\right), \quad (2)$$

$$\varphi_{xyz} = -\theta \exp\left(-\frac{|r_{xy}| + |2z - 1|}{2D}\right), \quad (3)$$

$$\dot{\varphi}_{xyz} = \begin{cases} \omega_{max} & \text{if } (2x - d_x)^2 + (2y - d_y)^2 + (2z - 1)^2 \leq d^2, \\ \omega_{min} & \text{if } (2x - d_x)^2 + (2y - d_y)^2 + (2z - 1)^2 > d^2, \end{cases}$$

where

$$\begin{aligned} r_{rot} &= \sqrt{(r_{xy})^2 + (z - 0.5)^2}, \quad r_{xy} = (x - 0.5) \cos(\psi) + (y - 0.5) \sin(\psi) + \frac{D}{2}, \\ d_x &= 1 + D \cos(\psi), \quad d_y = 1 + D \sin(\psi), \quad \theta = \text{atan2}(z - 0.5, r_{xy}), \\ \psi &= \text{atan2}(y - 0.5, x - 0.5), \quad x = i/N, \quad y = j/N, \quad z = k/N. \end{aligned}$$

The parameters $D, d \in (0, 1]$. $x, y, z \in [1/N, 1], \psi \in [-\pi, \pi]$.

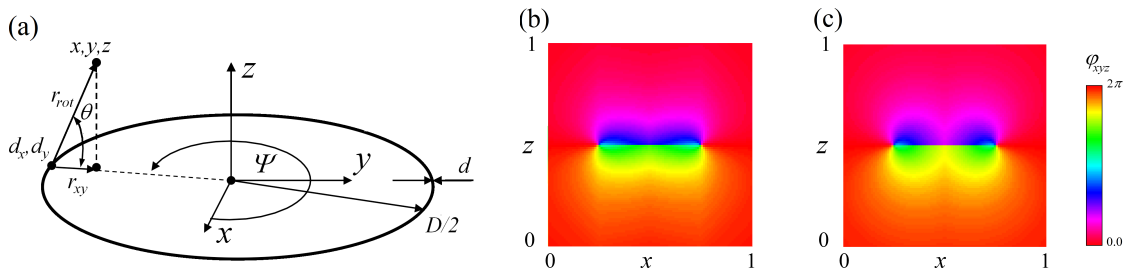


Figure 1. Schematic view of the construction of initial conditions (a). Phase cross-sections of initial conditions φ_{xyz} modulo 2π along $y=0.5$: (b) - type (2), (c) - type (3). Parameters $D = 0.5, d = 0.04, N = 100$.

The initial conditions (2), (3) describe the rotation of the phase φ_{xyz} around all axes tangent to the circle with diameter D in the plane $z = 0.5$. The schematic illustration of their construction is presented in Fig. 1(a). To satisfy the boundary conditions, the phase exponentially damps from the rotation center to the boundary. The fast damping to zero provides the same phase at large distances from the rotation center. The damping laws are different for (2) and (3). The analytic expression (2) yields a slower damping in the (x, y) plane and a faster damping in the z direction. The analytic expression (3) describes the symmetric damping around the rotation axis. A single scroll ring without phase damping satisfies periodic boundary conditions in the plane $z = 0.5$. The symmetric phase damping (3) is considered as the most simple case of damping law for the scroll rings. Figures 1(b) and 1(c) demonstrate the difference between the initial conditions (2) and (3) by the presentation of the cross-sections of the phase φ_{xyz} modulo 2π along $y = 0.5$ at the parameter values $D = 0.5, d = 0.04, N = 100$.

The value of the parameter ω_{max} is the maximal frequency of chimera's oscillators, ω_{min} is the frequency of the rest synchronized oscillators for any chimera states (not necessarily a scroll ring) obtained for fixed parameter values $\alpha, \epsilon, \mu, r, N$ of model (1), which can be obtained from the random initial condition at these parameter values. These parameters must be determined before starting the simulation procedure.

In this way, the initial conditions (2), (3) guarantee the generation of single scroll ring or toroid chimeras, as well as multiple scroll rings or other scroll wave chimeras. The scroll toroid chimeras must have minor diameter more than $1/N$.

Nevertheless, although the minor diameter of resulting scroll ring chimeras is determined largely by the parameter d , the value of the relative coupling radius $r = P/N$ has also a great influence on it.

Before starting the simulation of scroll ring and scroll toroid chimeras with expected major and minor diameters, we must preliminary calculate the parameter domains of model (1), where the patterns exist and are stable, by using proposed initial conditions. Such regions for the scroll ring chimeras in the parameter plane (α, μ) at $\epsilon = 0.05, r = 0.01, N = 200$ is presented in Fig. 2. These regions are similar to the stability regions for scroll ring chimeras obtained from the random initial conditions, but for another value of $r = 0.04$ (see Fig. 3(a) in [21]).

Our simulation shows that the scroll ring chimera states exist for any infinitely

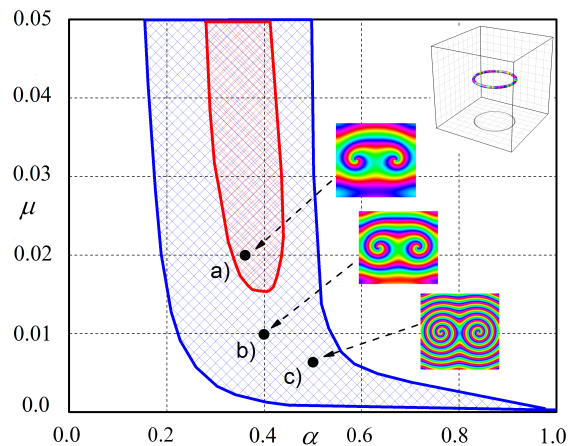


Figure 2. Stability regions for scroll ring chimeras in the parameter planes (α, μ) . Blue - scroll rings with the incoherent or partially coherent inner part, red - coherent rings. Snapshots of typical scroll ring chimeras and cross-sections of their phases φ_{xyz} along $y=0.5$ are shown in the insets. Parameters $\epsilon = 0.05, r = 0.01, N = 200$.

small coupling strength $\mu > 0$. Crossing the left and left bottom sides of the scroll ring stability region, all oscillators are synchronized. After crossing the right side of the region, the rings are destroyed with the generation of the chaotic oscillatory mode or their total synchronization.

The examples of typical scroll ring chimeras and their cross-sections in the insets of Fig. 2 at parameter point a) - c) demonstrate that the scroll waves are more densely twisted around the scroll ring chimeras with decreasing the parameter μ .

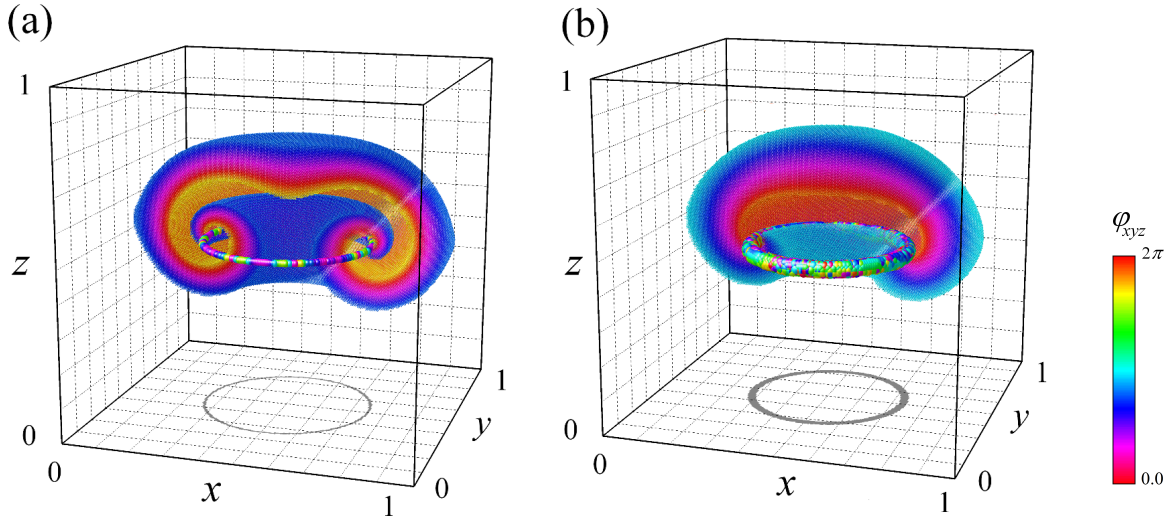


Figure 3. Phase snapshots of scroll ring and scroll toroid chimeras obtained from the initial conditions (2): (a) - scroll ring chimera ($\mu = 0.016, r = 0.01, d = 0.005$), (b) - scroll toroid chimera ($\mu = 0.01, r = 0.03, d = 0.08$). Common parameters $\alpha = 0.4, \epsilon = 0.05, D = 0.5, N = 200$. Simulation time $t = 10^5$. Half of the wave has been removed to permit the view of the scroll chimeras. Coordinates $x = i/N, y = j/N, z = k/N$. The space-time dynamics of the scroll ring and scroll toroid chimera states are illustrated by videos in supplemental data.

Figure 3 illustrates the results of simulation with the use of the initial condition (2) for scroll ring chimera (a) and for scroll toroid chimera (b) with major diameter of 0.5. In the case of scroll toroid chimera, its minor diameter is far more than $1/N$, which clearly seen in Fig. 3(b). In particular, the projection of the pattern onto the (x, y) plane confirms it. Here, we take $\omega_{max} = 0.06, \omega_{min} = -0.19$. In these figures, a half of the wave has been removed to permit one to better see the chimeras.

Scroll ring chimeras can have different inner structures of filaments and different dynamics of their oscillators that are characterized by the time-averaged frequencies $\bar{\omega}_{xyz}$ of their oscillators. The examples of scroll ring chimeras with coherent, partially coherent, and incoherent inner parts with the major diameter of 0.5 are presented in Fig. 4. Location of their parameter values in the parameter plane (α, μ) for these examples are indicated by black points a) - c) in Fig. 2.

In the case of a completely coherent scroll ring (Fig. 4(a)) all oscillators of the scroll ring chimera rotate with the same time-averaged frequency $\bar{\omega}_{xyz}$. The scroll ring chimera with partially coherent oscillatory organization has a segments of the same average frequency of scroll rings oscillators (green color) (Fig. 4(b)). Its ordered oscillator index

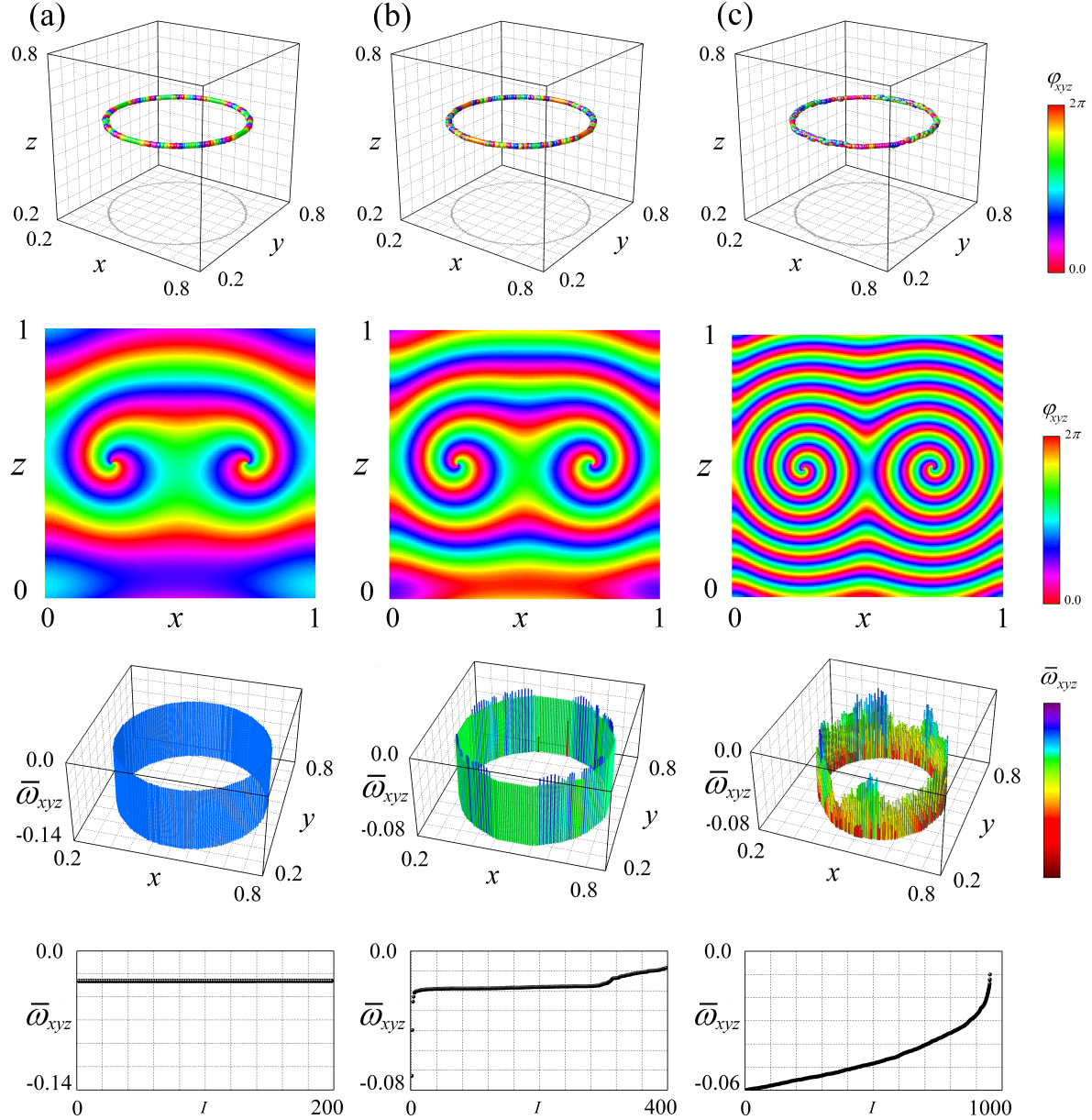


Figure 4. Examples of coherent, partially coherent, and incoherent scroll ring chimeras. Phase snapshots φ_{xyz} (upper row), their phase cross-sections along $y=0.5$, the average frequencies $\bar{\omega}_{xyz}$ (next two rows), ordered oscillator index (bottom row): (a) - coherent scroll ring chimera ($\alpha = 0.35, \mu = 0.02$), (b) - partially coherent scroll ring chimera ($\alpha = 0.4, \mu = 0.01$); (c) - incoherent scroll ring chimera ($\alpha = 0.5, \mu = 0.007$). Common parameters $r = 0.01, \epsilon = 0.05, N = 200$. Simulation time $t = 5 \times 10^4$, frequency averaging interval $\Delta T = 10^4$.

I has a long band for oscillators with the same average frequency $\bar{\omega}_{xyz}$. In the case of an incoherent scroll ring chimera, its average frequencies profile is chaotic (Fig. 4(c)). The dynamical complexity of the chimera state can be characterized by a number of positive Lyapunov exponents.

Lyapunov exponents λ_n characterize how the initial perturbations behave

themselves along the whole trajectory and are defined as the eigenvalues of a matrix

$$\Lambda = \lim_{t \rightarrow \infty} \frac{1}{2t} \log(Y(t)Y^T(t)),$$

where the matrix Y is a solution of the linearized differential equation $\dot{Y}(t) = J(t)Y(t)$ with the identity matrix as initial conditions, and $J(t)$ is a Jacobi matrix of system (1). Lyapunov exponents were estimated using the QR approach [27].

We suggest that, in the considered example (Fig. 4(c)), the scroll ring chimera has hyper-chaotic character with the huge number, more than one hundred, of positive Lyapunov exponents.

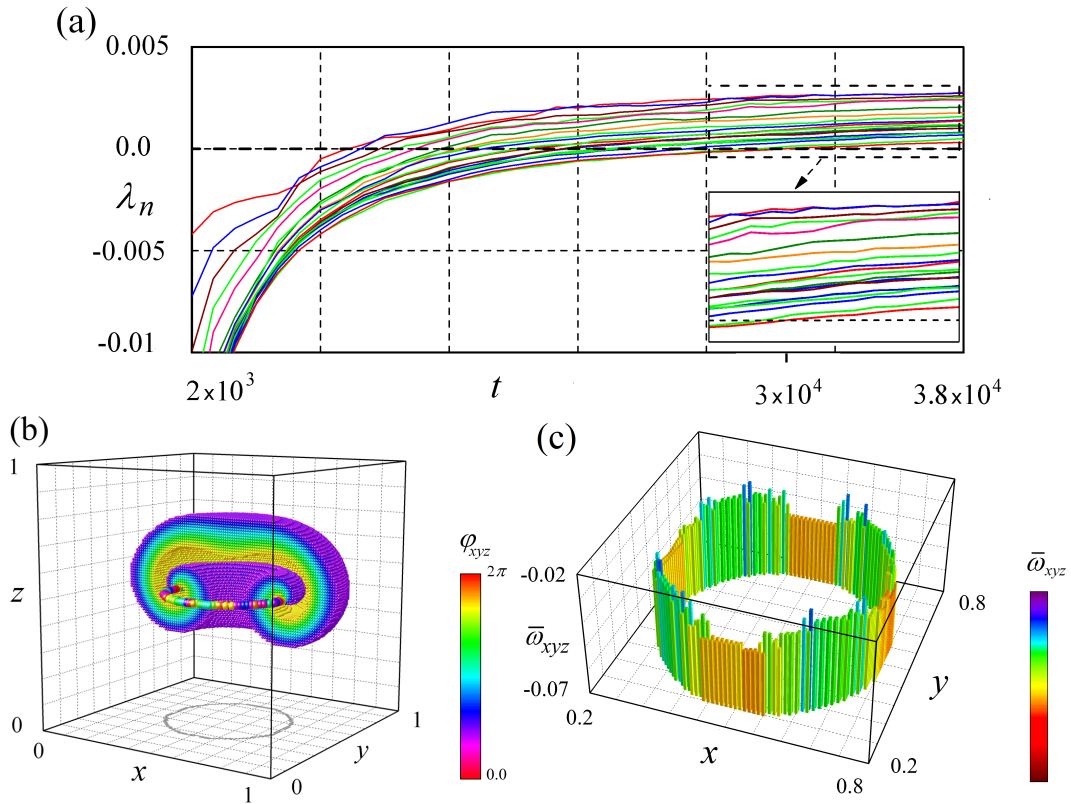


Figure 5. Lyapunov spectrum for 20 largest Lyapunov exponents (a) of the scroll ring chimera (b) and its average frequencies $\bar{\omega}_{xyz}$ (c) for the parameters $\alpha = 0.45, \mu = 0.01, \epsilon = 0.05, r = 0.02, D = 0.5, d = 0.01, N = 100$. Simulation time $t = 5 \times 10^4$, frequency averaging interval $\Delta T = 10^4$.

Figure 5 illustrates the Lyapunov spectrum of 20 largest Lyapunov exponents (a) of the scroll ring chimera (b) and its average frequencies $\bar{\omega}_{xyz}$ (c). At the time $t \approx 3 \times 10^4$, all 20 largest Lyapunov exponents become positive, confirming the hyper-chaotic character of this scroll ring chimera state.

We believe that if system (1) with dimension N increases, then it will be possible, using the initial conditions (2) and (3), to obtain different scroll ring chimeras including such ones with a stepwise profile with the average frequencies $\bar{\omega}_{xyz}$ similarly to the structure of spiral cores in the 2D Kuramoto model with inertia [24].

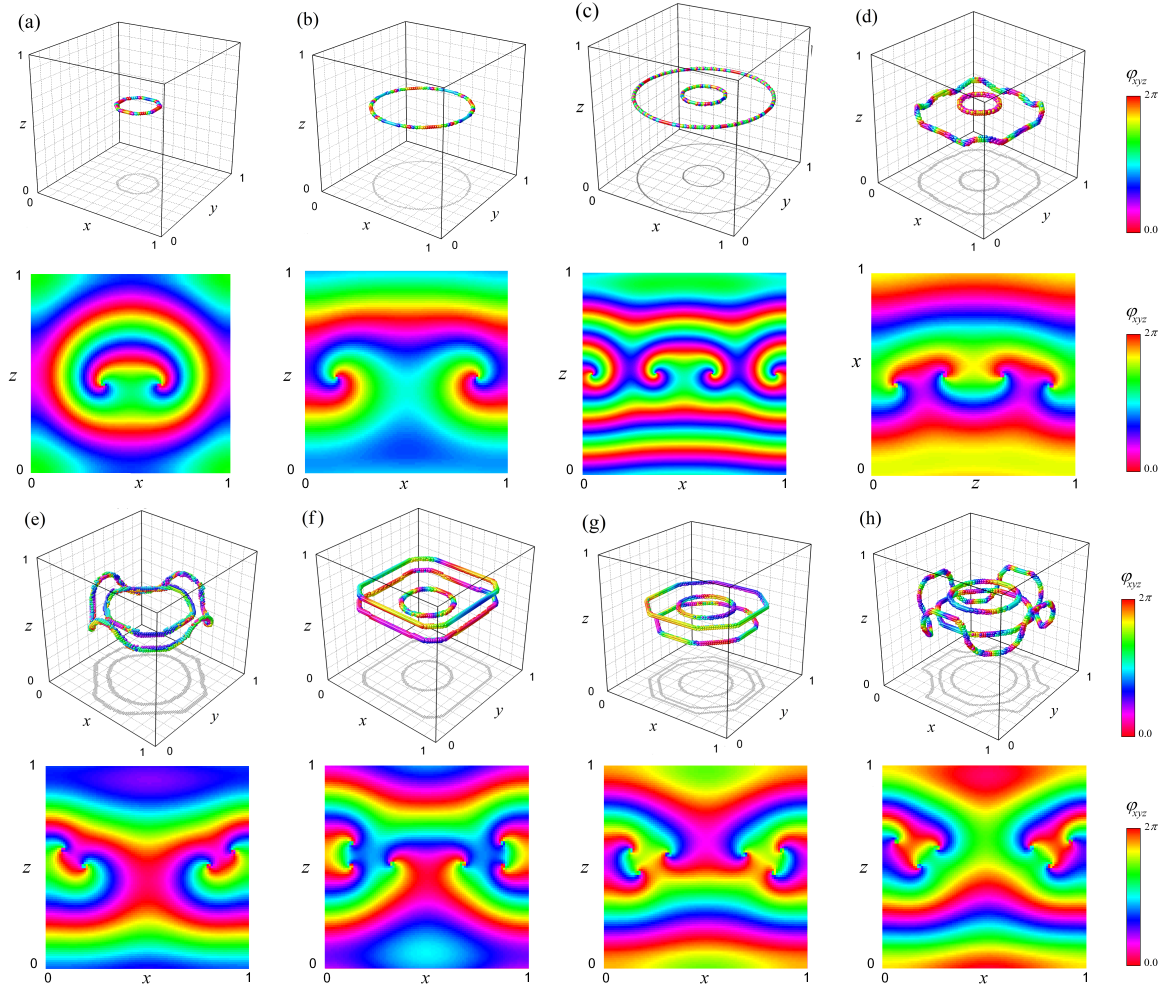


Figure 6. Examples of scroll ring chimeras generated by the initial conditions (2), (3). Phase distributions φ_{xyz} and their cross-sections along $y = 0.5$: (a) - scroll ring with a major diameter of 0.3 ($r = 0.02, D = 0.3, d = 0.01, N = 100$), (b) - scroll ring with a major diameter of 0.7 ($r = 0.02, D = 0.7, d = 0.01, N = 100$), (c) - double concentric scroll rings ($r = 0.02, D = 0.9, d = 0.005, N = 200$), (d) - double scroll rings with wave profile ($r = 0.03, D = 0.88, d = 0.1, N = 100$), (e) - double scroll rings with wave profile ($r = 0.03, D = 0.58, d = 0.2, N = 100$), (f) - three scroll rings ($r = 0.03, D = 0.66, d = 0.2, N = 100$), (g) - three scroll rings ($r = 0.03, D = 0.64, d = 0.22, N = 100$), (h) - three scroll rings with wave profile ($r = 0.03, D = 0.74, d = 0.24, N = 100$). Common parameters $\alpha = 0.38, \mu = 0.02, \epsilon = 0.05$. Simulation time $t = 5 \times 10^4$. Coordinates $x = i/N, y = j/N, z = k/N$.

The initial conditions (2) and (3) can generate single scroll ring or scroll toroid chimeras, as well as multiple scroll patterns with different major and minor diameters. Some filaments of them are transformed into polygons or can have a wave profile in the z direction.

In Fig. 6, a few examples of scroll ring chimeras, as a result of the simulation with the use of the initial conditions (2) and (3), are presented for the fixed parameters $\alpha = 0.38, \mu = 0.02, \epsilon = 0.05$. The initial conditions are taken in the form of (2) for Fig. 6(a, b, e, h) and in the form of (3) for Fig. 6(c, d, f, g).

We note that the proposed initial conditions (2), (3) can be used for any values of

N of system (1). We present the results of their application in the cases of $N = 100$ and $N = 200$ in Fig. 6(a, b, d-h) and Fig. 6(c), respectively.

In addition to the example of a scroll ring chimera with the major diameter of 0.5 (Fig 3(a)), the examples of scroll ring chimeras with the major diameter of 0.3 and 0.7 are presented in Fig. 6(a) ($D = 0.3, d = 0.01$) and Fig. 6(b) ($D = 0.7, d = 0.01$), respectively.

The example of a multiple scroll ring chimera obtained from the proposed initial conditions is given in Fig. 6(c-h): (c) - double concentric scroll rings ($D = 0.9, d = 0.005$), (d) - double scroll rings with wave profile ($D = 0.88, d = 0.1$), (e) - double scroll rings with wave profile ($D = 0.58, d = 0.2$), (f) - three scroll rings ($D = 0.66, d = 0.2$), (g) - three scroll rings with polygon profile ($D = 0.64, d = 0.22$), (h) - three scroll rings with wave profile ($D = 0.74, d = 0.24$). Multiple scroll patterns in the form of polygons or with wave profile can be generated by initial conditions (2), (3) with parameter $d > 0.09$. So, using the initial conditions (2), (3) with different parameters D and d , we can obtain as many multiple scroll wave ring and toroid chimeras as we simulate.

Our simulation shows that all scroll ring chimeras obtained in this way are stable with respect to perturbations of the phase variables φ_{xyz} and frequencies ω_{xyz} by a uniformly distributed noise. The perturbed scroll ring chimeras still exist and retain their shapes under a perturbation of the amplitude less than 0.5 at the parameters $\alpha = 0.38, r = 0.02, \mu = 0.1, \epsilon = 0.05$, and $N = 200$. Stronger perturbations lead to changing the shapes of scroll ring chimeras, their destruction with complete oscillatory synchronization, or the creation of different types of scroll wave chimera states. Moreover, if the disturbed scroll ring lies in the parameter region, where solitary states exist, the perturbation can give rise to another scroll ring chimera with solitary clouds [21]. Due to these properties, we can build complex patterns in the system (1), for example, consisting of scroll ring chimeras and other patterns.

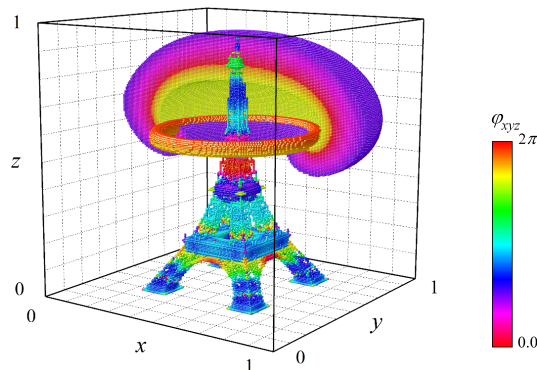


Figure 7. Phase snapshot of the 3D image of the Eiffel Tower with a scroll ring chimera. The parameters $\alpha = 0.4, r = 0.04, \mu = 0.1, \epsilon = 0.05, D = 0.5, d = 0.005, N = 200$. A half of the wave has been removed to permit the view of the scroll ring chimera and the Eiffel Tower image. The space-time dynamics of the chimera states are illustrated by video in supplemental data.

Finally, to illustrate the possibility of the coexistence of the scroll rings with other patterns in the 3D oscillatory network, we present the Eiffel tower image surrounded

by scroll ring chimeras in Fig. 7. The initial conditions for the patterns were built, by using the Eiffel tower solitary oscillators and the initial conditions (2) for a scroll ring chimera with the parameters $D = 0.5$ and $d = 0.005$ placed in a 3D cube at $z = 0.6$. Distribution of scroll ring chimera oscillators was taken as the base for initial conditions. Then the model of Eiffel tower for the 3D printing was used as a spatial template for the placement of solitary oscillators inside a scroll ring chimera. Model for 3D printing contains spatial coordinates of voxels that should be filled with plastic. These voxel coordinates were scaled to the size of the scroll ring chimera system and used for placement of solitary oscillators inside a system with a scroll ring chimera. The average frequency of solitary oscillators was selected to be close to the average frequency of scroll ring oscillators. Due to properties of solitary states [21], there is no interference between solitary oscillators of the Eiffel tower and the oscillators of a scroll ring chimera after several hundreds time units transient. This image is a stable solution of the 3D Kuramoto model with inertia (1).

The scroll ring has a ring-like filament and is related to a scroll wave and a toroidal vortex/swirl as a special case. Scroll rings also appear in a variety of experimentally observed effects and as solutions of the equations of realistic mathematical models. Equations similar to (1) appear in different problems of hydrodynamics, aerodynamics, and plasma dynamics and are related to flows, flames, superfluidity etc. (see, e.g., [28–30]). The fibrillation of cardiac tissue is described by scroll ring dynamics, and some chemical reactions lead to the propagation of scroll ring reagents' concentration waves. The appearance of scroll rings and other related phenomena are sometimes considered as harmful (flow turbulence, fibrillation) and, sometimes, as useful (combustion chambers, chemical reactions). Knowledge of conditions, where scroll rings can and cannot exist, may be inculcated in practice: design of new devices, therapies, technologies.

Acknowledgments

The authors are grateful to the Ukrainian Grid Infrastructure for providing the computing cluster resources and the parallel and distributed software used during this work.

References

- [1] A. Winfree. *Science* **181**, pp. 937–939, (1973).
- [2] A. Winfree. *Science* **175**, pp. 634–636, (1972).
- [3] A. Medvinsky, A. Panfilov, A. Pertsov. Springer, Heidelberg, p. 195, (1984).
- [4] A. Winfree, S. Strogatz. *Physica D*, pp. 35–49, (1983).
- [5] A. Panfilov, A. Rudenko, A. N. *Physica D*, **28**, 215, (1987).
- [6] A. Winfree. *The Geometry of Biological Time*, Springer, Berlin, (2001).
- [7] E. Cherry, F. Fenton. *New J. Phys.* 10 125016 (2008).
- [8] Z. Qua, G. Hub, A. Garfinkel, J. Weissad. *Physics Reports* **543**, Issue 2, 10, pp. 61–162, (2014).
- [9] V. Biktashev, I. Biktasheva. *Engineering of Chemical Complexity II*, pp. 221 — 238, (2014).

- [10] J. Tetz, H. Engel, O. Steinbock. *New J. Phys.* **17**, 093043, (2015).
- [11] Y. Kuramoto. *Nonl. Dyn. and Chaos*, CRC Press, pp. 209 – 227, (2002).
- [12] Y. Kuramoto, D. Battogtokh. *Nonlinear Phenom. Complex Syst.* **5**, pp. 380 – 385, (2002).
- [13] D. Abrams, S. Strogatz. *Phys. Rev. Lett.*, **93**, 174102, (2004).
- [14] F. Parastesh, S. Jafari, H. Azarnoush, Z. Shahriari, Z. Wang, S. Boccaletti, M. Perc. *Physics Reports*, **898**, pp. 1–114 (2021).
- [15] Yu. Maistrenko, O. Sudakov, O. Osiv, V. Maistrenko. *New Journal of Physics*, **17**, 073037, (2015).
- [16] H. Lau, J. Davidsen. *Phys. Rev.E*, **94**, 010204(R), (2016).
- [17] V. Maistrenko, O. Sudakov, O. Osiv, Yu. Maistrenko. *EPJ ST*, V. **226**, Issue 9, (2017).
- [18] T. Kasimatis, J. Hizanidis, A. Provata. *Phys. Rev. E* **97**, 052213, (2018).
- [19] S. Kundu, B.K. Bera, B, D. Ghosh, M. Lakshmanan. *Phys. Rev. E*, **99(2)**, (2019).
- [20] O.Omel'chenko, E.Knobloch. *New Journal of Physics*, **21**, (2019).
- [21] V. Maistrenko, O. Sudakov, O. Osiv. *Chaos* **30**, 063113 (2020).
- [22] P. Jaros, Yu. Maistrenko, T. Kapitaniak. *Phys. Rev. E* **91**, 022907 (2015).
- [23] P. Jaros, S. Brezetsky, R. Levchenko, D. Dudkowski, T. Kapitaniak, Yu. Maistrenko. *Chaos* **28**, 011103 (2018).
- [24] V. Maistrenko, O. Sudakov, Yu. Maistrenko. *Eur. Phys. J. Spec. Top.* **229**, 2327–2340 (2020).
- [25] A. Salnikov, R. Levchenko, O. Sudakov. *Proc. 6th IEEE (IDAACS)*, pp. 198 – 202 (2011).
- [26] O. Sudakov, A. Cherederchuk, V. Maistrenko. *Proc. 9th IEEE (IDAACS)*, pp. 311 - 316 (2017).
- [27] L. Dieci, M. Jolly, E. Vleck. *J. Comput. Nonlinear Dynam.* Jan 2011, **6(1)**, 011003 (2011).
- [28] D. Dennis, C. Seraudie, R. Poole. *Phys. of fluids* **26**, 053602 (2014).
- [29] Y. Huang, V. Yang, V. Proc. *Combustion Institute* **30**, 1775-1782 (2005).
- [30] N. Guenther, P. Massignan, A. Fetter. *Phys. Rev. A*, **101**, 053606 (2020).